Disequilibrium and macrosegregation during solidification of a binary melt

Ross C. Kerr, Andrew W. Woods, M. Grae Worster & Herbert E. Huppert

Department of Applied Mathematics and Theoretical Physics, University of Cambridge, Silver Street, Cambridge CB3 9EW, UK

The crystallization of a liquid mixture in the presence of natural convection is an important problem in geophysics and metallurgy. Simple aqueous solutions may be used as analogue systems to study this process. Both theory and experiment reveal that convective motions in the fluid are important in determining both the rate of solidification and the development of compositional stratification in the solid. Moreover, convection may result in solidification in regions other than near the boundary at which cooling is imposed.

WHEN a melt of two or more components solidifies, the composition of the resulting solid is generally different from that of the melt. For example, salt water in the oceans freezes to form almost pure ice, and the partial solidification of a melt containing comparable quantities of germanium and gallium produces almost pure germanium. This compositional difference between the solid and melt indicates that the composition of the fluid in the near vicinity of the crystallization front differs from that in the bulk of the fluid, which generally implies that the density is also different. Contrasts in density can drive intense convective flows. Fluid mechanical effects should thus play a large role in solidifying systems, whether the final products are small-scale semiconductor crystals or the solid inner core of the Earth.

In the simple but fundamental situation of the cooling of an initially homogeneous melt at a single horizontal boundary, six different flow regimes have been identified[1] which depend on whether the thermal field results from cooling at either an upper or lower boundary to the melt and whether the fluid released on solidification has a greater, a lesser, or the same density as the melt. Building on previous investigations[2], we concentrate here on cooling, at an upper horizontal boundary, a melt that releases less-dense fluid on solidification. We highlight some novel interactions between fluid convection and crystallization. Identifying each new effect in turn, we present mathematical models to quantify the outcome in each case and describe its significance. Our theoretical predictions compare well with results from our laboratory experiments in which we use various aqueous solutions such as isopropanol and sodium sulphate. These are easy to handle in the laboratory and mimic the behaviour of a wide variety of binary alloys with which it is much more difficult to conduct controlled experiments.

The theoretical development incorporates the analysis of regions where solid dendritic crystals and melt coexist as a 'mushy' region[3,4]. Figure 1 shows photographs of a mushy region consisting of solid ice and isopropanol-enriched water. Our aim is to calculate the rate of growth of the mushy layer and the variation in the fraction of solid ice within it. We first consider the mushy layer to grow under conditions of thermodynamic equilibrium. This leads to results in good, but not perfect, agreement with our experimental observations. The agreement is improved by permitting the melt to depart from thermodynamic equilibrium and to become supersaturated. In addition, this leads to an explanation of solidification at the floor, which occurs even though the system is cooled at the roof. Only if the temperature at the roof is less than the eutectic temperature of the melt can complete solidification take place. In this case, compositional zonation of the solid is observed. This is a consequence of crystallization at the floor, which releases solvent into the melt and results in an evolution of the composition of the melt.

The model system and equations

Figure 2*a* illustrates the model system that forms the basis for our study. A rectangular container is filled with a two-component melt (or solution) of initially uniform composition C_0 and temperature T_0. At the start ($t=0$) the upper boundary is instantaneously cooled to, and subsequently maintained at, a temperature T_b that is lower than the liquidus temperature $T_L(C_0)$ of the solution. All the other boundaries are considered to be thermally insulated.

In our first investigations T_b was greater than than the eutectic temperature T_e of the binary system. The melt could therefore

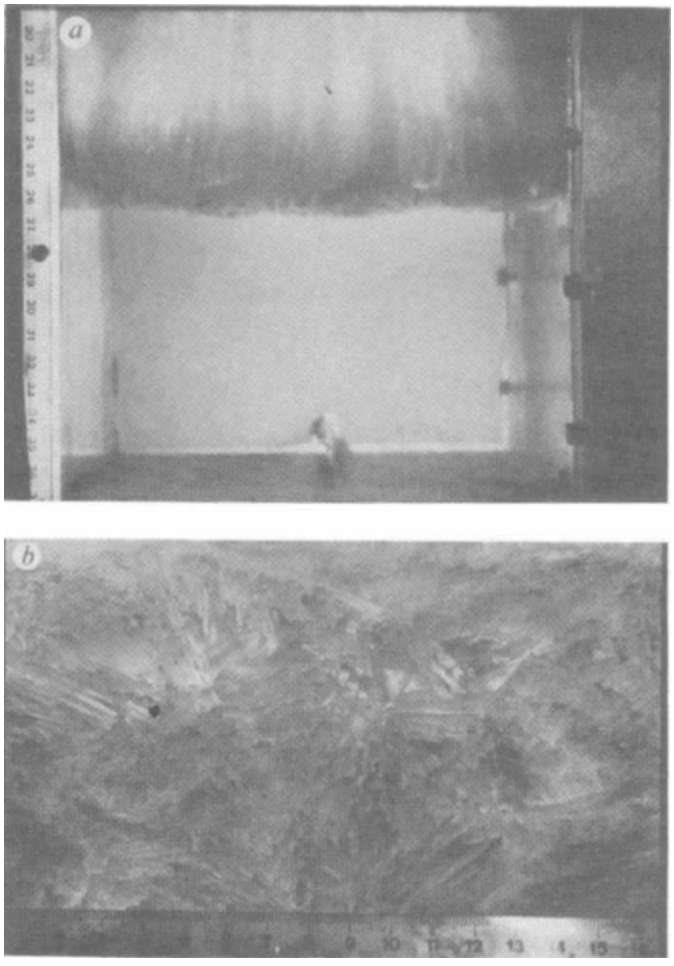

FIG. 1 Photographs of the mushy layer in an isopropanol experiment. *a*, A side view showing that the interface with the melt is approximately flat. *b*, A close-up view normal to the interface, showing the closely-spaced, plate-like ice crystals. This fine-scale structure allows the mushy layer to be treated theoretically as a continuum.

never be completely solidfied. The behaviour that occurs if the fluid released on solidification is less dense than the melt is illustrated by our laboratory experiments with mixtures of isopropanol and water. Ice formed at the upper boundary and grew downwards in thin plates to form the mushy layer depicted in Fig. 1. The fluid in the interstices of the mushy layer was enriched in isopropanol as a result of the selective freezing of water to form ice from the binary melt. The enriched isopropanol solution was less dense than the original solution and remained stagnant within the mushy layer. Below the mushy layer we observed turbulent thermal convection of the fluid in response to the cooling from above. This convection played an important role in the subsequent evolution of the system. The experiments were continued until the lower edge of the mushy layer had descended to within a centimetre or so from the base of the tank, which took ~25 hours. The position of the mush-liquid interface and the temperature of the well mixed liquid region were monitored at intervals throughout the experiments.

To evaluate the experimental results and apply our findings generally to other systems, we have developed a mathematical model based on our understanding of the physical processes involved in the laboratory experiments. Equations governing heat and mass conservation within the mushy layer are derived from ref. 5. Transport of heat is governed by thermal diffusion and is described by

$$c_m \frac{\partial T}{\partial t} = \frac{\partial}{\partial z}\left(k_m \frac{\partial T}{\partial z}\right) + \mathscr{L}_\beta \frac{\partial \phi}{\partial t} \tag{1}$$

where T is the local temperature and ϕ the local volume fraction of solid dendrites. Changes in ϕ result in an internal release of latent heat which must be conducted through the mushy layer. The thermodynamic parameters are the specific heat per unit volume c, the thermal conductivity k and the latent heat per unit volume of solid $\mathscr{L}$. Subscripts β, m and later l denote properties of the solid phase forming the dendrites, the mushy layer and the liquid respectively. We evaluate the thermal properties of multi-phase media by equating them to local averages, weighted by the volume fraction, of the properties of the constituent phases. So, for example, the specific heat per unit volume and the thermal conductivity of the mushy layer are given by

$$c_m = \phi c_\beta + (1-\phi)c_l \tag{2}$$

and

$$k_m = \phi k_\beta + (1-\phi)k_l \tag{3}$$

Whereas equation (2) is exact, equation (3) is only approximate because conductivity depends on the microscopic morphology. However, equation (3) is an exact expression for a laminated material when the thermal gradient is aligned with the laminates[6], and it has led to excellent results in previous analyses of stagnant mushy layers[1,5].

Huppert and Worster[1], and Worster[5] demonstrate that the depth of a stagnant mushy layer is determined principally by thermal balances. Therefore, as the thermal diffusivity is typically much greater than the solutal diffusivity, we assume that vertical diffusion of solute is negligible. Conservation of solute in the mushy layer can then be expressed by a differential form of the Scheil equation[3],

$$(1-\phi)\frac{\partial C}{\partial t} = (C - C_\beta)\frac{\partial \phi}{\partial t} \tag{4}$$

where C is the concentration of the interstitial liquid and C_β is the uniform concentration of the solid dendrites. Equation (4) is readily integrated to show that the bulk, horizontally averaged composition $C_H = (1-\phi)(C - C_\beta)$ is a function of z only. Finally, we couple equations (1) and (4) by using the linearized liquidus relationship.

$$T = T_L(C) \equiv T_L(C_0) + \Gamma(C - C_0) \tag{5}$$

where Γ is a constant, on the assumption that the mushy layer is in local thermodynamic equilibrium.

Conservation of heat across the thermal boundary layer at the moving interface between mush and liquid requires that

$$[c_l(T_l - T_i) + \mathscr{L}_\beta \phi]\dot{h}_i = k_m \left.\frac{\partial T}{\partial z}\right|_{z=h_i-} - F_T \tag{6}$$

where $h_i(t)$ is the position of the interface, T_i is the temperature there and F_T is the convective heat flux from the liquid to the mushy region. Conservation of heat in the region of well mixed liquid is expressed by

$$c_l(H - h_i)\dot{T}_l = -F_T \tag{7}$$

where H is the initial depth of the liquid. The heat flux F_T is approximated by the well-known semi-empirical relationship for turbulent convective heat transfer across a horizontal surface

$$F_T = (2^{4/3}\lambda)k_l\left(\frac{\alpha g}{\kappa_l \nu}\right)^{1/3}(T_l - T_i)^{4/3} \tag{8}$$

where g is the acceleration due to gravity, α is the coefficient of thermal expansion of the liquid, κ_l is its thermal diffusivity, ν is its kinematic viscosity and λ is an empirical constant. This relationship, which is often expressed in the dimensionless form $Nu \propto Ra^{1/3}$, where Nu is the Nusselt number and Ra is the Rayleigh number, can be derived from the assumption that the turbulent heat flux is independent of the depth of the convecting region[7].

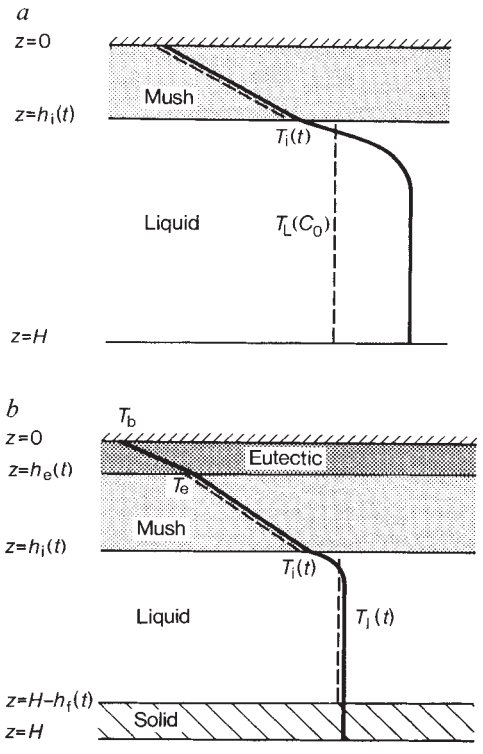

FIG. 2 Definition sketches of two models (*a*, *b*) for the growth of a mushy layer below a cold horizontal boundary maintained at a fixed temperature T_b. Throughout the mushy layer, the temperature (solid line) is constrained to equal the liquidus temperature (dashed line) of the interstitial melt. The interfacial temperature T_i is less than the equilibrium freezing temperature of the melt $T_L(C_0)$. Turbulent convection of the melt keeps its temperature uniform. Diagram *a* corresponds to our experiments with isopropanol. The boundary temperature is greater than the eutectic temperature T_e and a mushy layer forms adjacent to the cooled boundary only. In *b* there are two additional layers. The first is a layer of composite solid that grows on the roof when $T_b < T_e$. The second, which usually appears once the melt temperature T_l reaches $T_L(C_0)$, is a solid layer of crystals that grows on the base at a rate sufficient to keep the melt on the liquidus. The temperature within the basal solid is taken to be equal to T_i.

To complete the model we adopt the condition of marginal equilibrium[5], which states that the temperature gradient in the boundary layer in the liquid ahead of the mush-liquid interface is equal to the gradient of the local liquidus temperature. This condition, combined with conservation of solute at the mush-liquid interface, leads to

$$\phi = 0, \quad C = C_0 \quad (\text{at } z = h_i) \qquad (9a, b)$$

in the limit of zero solute diffusivity. We note that equations (9*b*) and (5) imply that

$$T_i = T_L(C_0) \qquad (10)$$

whereas equations (9*b*), (4) and its integral imply that the bulk, horizontally averaged, composition C_H throughout the mushy layer is equal to the initial concentration C_0. The solid fraction is thus given by

$$\phi = \frac{C_0 - C}{C_\beta - C} \qquad (11)$$

It is instructive and useful to note that equations (1)-(5) can be combined into the nonlinear diffusion equation

$$\left[c_m + \frac{\mathscr{L}_\beta}{\Gamma} \frac{1-\phi}{C_\beta - C} \right] \frac{\partial T}{\partial t} = \frac{\partial}{\partial z}\left(k_m \frac{\partial T}{\partial z} \right) \qquad (12)$$

which shows that the release of latent heat acts simply to increase the thermal inertia of the mushy layer.

This system of equations was integrated numerically to determine the evolution of h_i and T_i. Figure 3 shows the results which are compared with data from the experiments with isopropanol. Very good agreement is found between theory and experiment for the growth of the mushy layer (Fig. 3*a*) and the cooling rate of the solution (Fig. 3*b*). The data show, however, that the temperature of the solution fell below the liquidus temperature during the course of each experiment. Such supersaturation, which cannot be accounted for with an equilibrium model, can have extremely important consequences for the evolution of the system, as we demonstrate below.

Disequilibrium

Crystal growth is necessarily a non-equilibrium process; some level of supersaturation must exist in the vicinity of a growing crystal interface to drive solidification. Usually the departures from equilibrium are small and good predictions of growth rates can be made by assuming that the system evolves through equilibrium states, as we have just demonstrated. A more accurate formulation of crystal growth takes account of the interfacial kinetics involved by recognizing that the rate of growth is a function of the local supersaturation[8,9]. We replace the equilibrium assumption leading to equation (10) by the simple linear relationship

$$\dot{h}_i = \mathscr{G}(T_L - T_i) \qquad (13)$$

where T_L is the liquidus temperature at the interface and $\mathscr{G}$ is a constant. The interface temperature is now less than T_L and $C_i < C_0$. Correspondingly, as there is still no solute flux across the interface, the solid fraction at the interface, given by equation (11) with $C = C_i$, is greater than zero[9]. By measuring carefully during many experiments the evolution of the depth of the mushy layer $h_i(t)$ and the temperature at the interface T_i, using a 1-mm bead thermistor, we have confirmed equation (13) for the water-isopropanol system for supersaturations $T_L - T_i$ up to 3 °C and measured $\mathscr{G}$ as $\sim 2.2 \times 10^{-4}$ cm s^{-1} °C^{-1}.

The kinetic growth law, equation (13), gives a timescale $\tau_{\mathscr{G}} = H/\mathscr{G}(T_L - T_b)$ associated with disequilibrium that can be compared with the timescale for thermal diffusion, $\tau_\kappa = H^2/\kappa$. The ratio $\varepsilon = \tau_{\mathscr{G}}/\tau_\kappa$ is typically very small; for example, it is 1.2×10^{-2} in our experiments with isopropanol. This indicates that when diffusion is the only transport process[1,5], departures from equilibrium are negligible except at very early times, of order $\tau_{\mathscr{G}} = \varepsilon \tau_\kappa$, compared with the solidification time, which is of order τ_κ. We

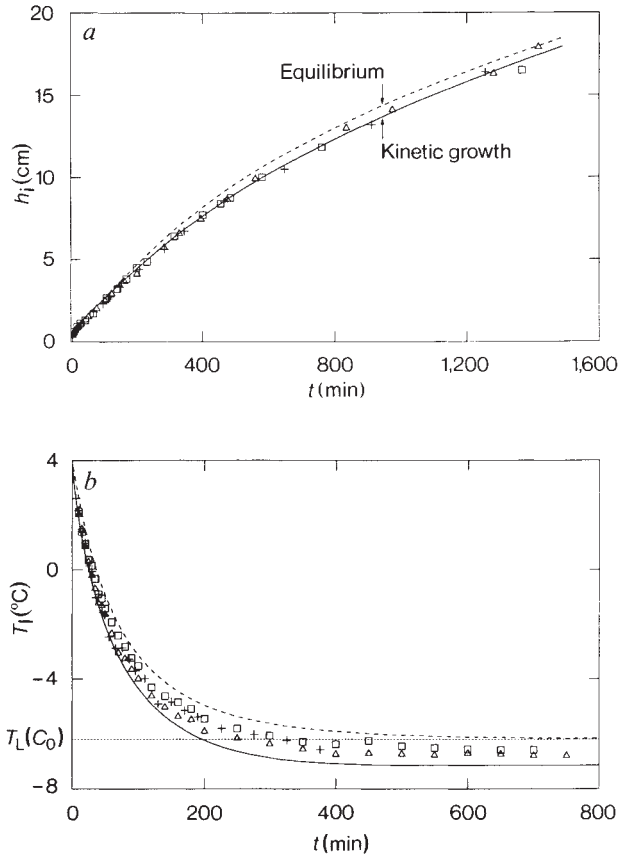

FIG. 3 *a*, The depth of the mushy layer h_i; *b*, the temperature of the solution T_i versus time including data obtained from isopropanol experiments in which $T_b = -25$ °C, $C_0 = 83.2$ wt% H_2O and $T_0 = 4.0$ °C. The height of the tank $H = 18.8$ cm. The dashed upper curve was calculated by using the equilibrium assumption that the interface temperature T_i is equal to the initial liquidus temperature of the solution $T_L(C_0)$. The solid lower curve was calculated by using the kinetic growth law, equation (13), to determine T_i, and gives a better fit to the data. The horizontal dotted line in *b* indicates the liquidus temperature of the solution (−6.2 °C). In the calculations $c_\beta = 1.832$ J cm^{-3} °C^{-1}, $c_l = 3.912$ J cm^{-3} °C^{-1}, $k_\beta = 0.022$ W cm^{-1} °C^{-1}, $k_l = 0.0037$ W cm^{-1} °C^{-1}, $\mathscr{L}_\beta = 306$ J cm^{-3}, $\nu = 0.057$ cm^2 s^{-1}, $\lambda = 0.056$ and the liquidus was represented by $T_L = -6.2 + 0.65(C - 83.2)$, where C is in wt% H_2O and T_L is in °C. All these values were determined from published data[20-25]. Our own measurements of α suggested $\alpha = (2.25 + 0.15T) \times 10^{-4}$ °C^{-1}, where T, in °C, was taken to be the mean of T_i and T_l.

shall see, however, that these small departures are important when coupled with convection of the melt.

The non-equilibrium model obtained by employing equation (13) rather than equation (9) is seen in Fig. 3*a* to give excellent agreement with experimental data for the growth of the ice. It also accounts for the occurrence of supersaturation in the liquid region after ~200 min. Note, however, that, owing to heat gain from the laboratory, there is a slight discrepancy between the predicted and experimentally observed results for the level of supersaturation.

Secondary crystallization

The experiments with mixtures of water and isopropanol were metastable for much of their evolution. That is, had there been sites for nucleation within the supersaturated liquid region then crystals could have grown anywhere in that region in addition to the crystals growing within the mushy layer. Such secondary crystallization has been observed, both by us and by previous authors[2], in laboratory experiments with various aqueous solutions. Figure 4 shows photographs of one of our experiments using sodium sulphate. In all these cases the solid forming the

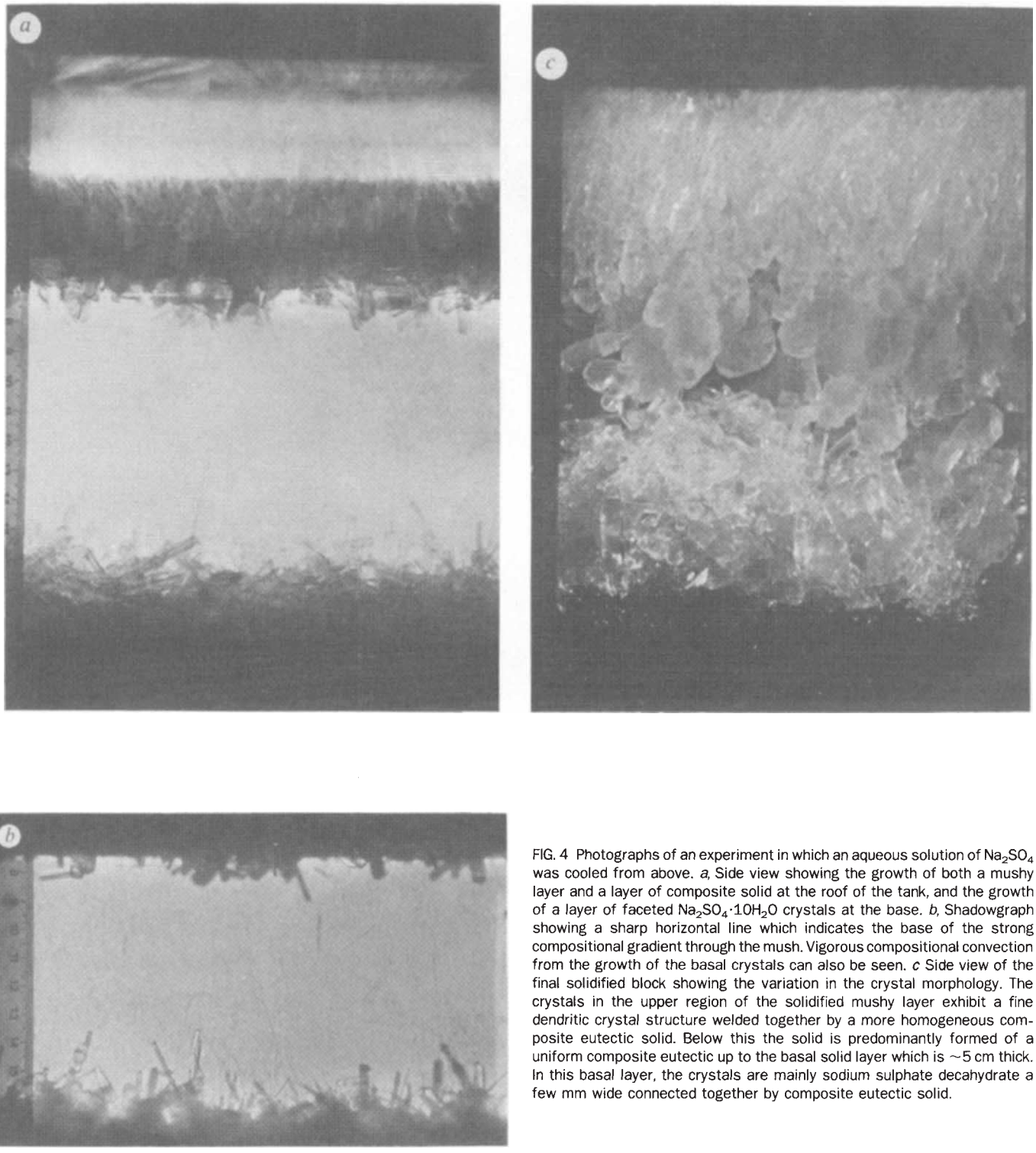

FIG. 4 Photographs of an experiment in which an aqueous solution of Na_2SO_4 was cooled from above. *a*, Side view showing the growth of both a mushy layer and a layer of composite solid at the roof of the tank, and the growth of a layer of faceted $Na_2SO_4 \cdot 10H_2O$ crystals at the base. *b*, Shadowgraph showing a sharp horizontal line which indicates the base of the strong compositional gradient through the mush. Vigorous compositional convection from the growth of the basal crystals can also be seen. *c* Side view of the final solidified block showing the variation in the crystal morphology. The crystals in the upper region of the solidified mushy layer exhibit a fine dendritic crystal structure welded together by a more homogeneous composite eutectic solid. Below this the solid is predominantly formed of a uniform composite eutectic up to the basal solid layer which is ~5 cm thick. In this basal layer, the crystals are mainly sodium sulphate decahydrate a few mm wide connected together by composite eutectic solid.

dendrites in the mushy layer was denser than the solution, and nucleation sites for crystallization may have been provided by a few small crystals that settled from the mushy layer.

The crystallization at the floor depleted the melt of solute locally to leave a buoyant residual liquid which caused compositional convection of the whole liquid region. The convection of solvent away from the growing crystals allowed for very efficient growth into the supersaturated liquid which we model by assuming that the crystals grew sufficiently rapidly to restore thermodynamic equilibrium to the liquid. This gives an upper bound on the rate of growth of the crystals on the floor, but we shall see that in fact it gives a good approximation for the observed growth. There is still a kinetic undercooling at the interface between mush and liquid as illustrated in the temperature profile of Fig. 2*b*.

If the crystals on the floor are assumed to occupy a solid layer of thickness $h_f(t)$ then global conservation of solute demands that

$$\dot{h}_f = \frac{H - h_i - h_f}{C_\beta - C_l}\dot{C}_l \tag{14}$$

where C_l is the composition, now changing, of the liquid region. Our assumption that the secondary crystal growth restores equilibrium to the convecting liquid can be expressed by

$$T_i = T_L(C_l) \tag{15}$$

and the latent heat released modifies equation (7), which becomes

$$\mathscr{L}_\beta \dot{h}_f - c_l(H - h_i - h_f)\dot{T}_l - c_\beta h_f \dot{T}_l = F_T \tag{16}$$

Although the release of solvent by the secondary crystal growth has an obvious direct effect on the liquid region, it also has an indirect effect on the evolution of the mushy layer. Even though there is no flux of solvent across the interface between mush and liquid, the changing composition of the liquid region means that the composition of the solution incorporated into the advancing mushy layer decreases with time. Consequently, the bulk composition of the mushy layer (including both liquid and solid phases) is a function of height. In fact, as we have neglected vertical transport of solute within the mushy layer, the bulk, horizontally averaged, composition $C_H(z)$ is given simply by the composition that the liquid region had at time t_i when the position of the interface between mush and liquid h_i was equal to z. That is,

$$C_H(z) = C_l(t_i) \quad \text{where } h_i(t_i) = z \tag{17}$$

One effect of the variation in $C_H(z)$ is to alter the solid fraction within the mushy layer

$$\phi = \frac{C_H(z) - C}{C_\beta - C} \tag{18}$$

which affects both the thermal properties given by equations (2) and (3) and the internal release of latent heat as expressed by equation (12). These changes all affect the rates of evolution of the system.

Compositional stratification

A more important consequence of the secondary solidification is that it provides an explanation for the compositional stratification that is often observed when binary melts are completely solidified. To investigate this effect quantitatively we carried out experimental and theoretical investigations of systems in which the upper cooled boundary was maintained at a temperature T_b that was lower than the eutectic temperature T_e. Figure 2*b* shows a schematic diagram of such a system. A composite solid made up of crystals of the two pure end members of composition C_α and C_β occupies the region $0 \leq z < h_e(t)$. Heat transfer across the layer occurs solely by conduction. At very early times $T_i < T_e$ and there is no mushy layer. For most of the evolution, however, the temperature in this composite

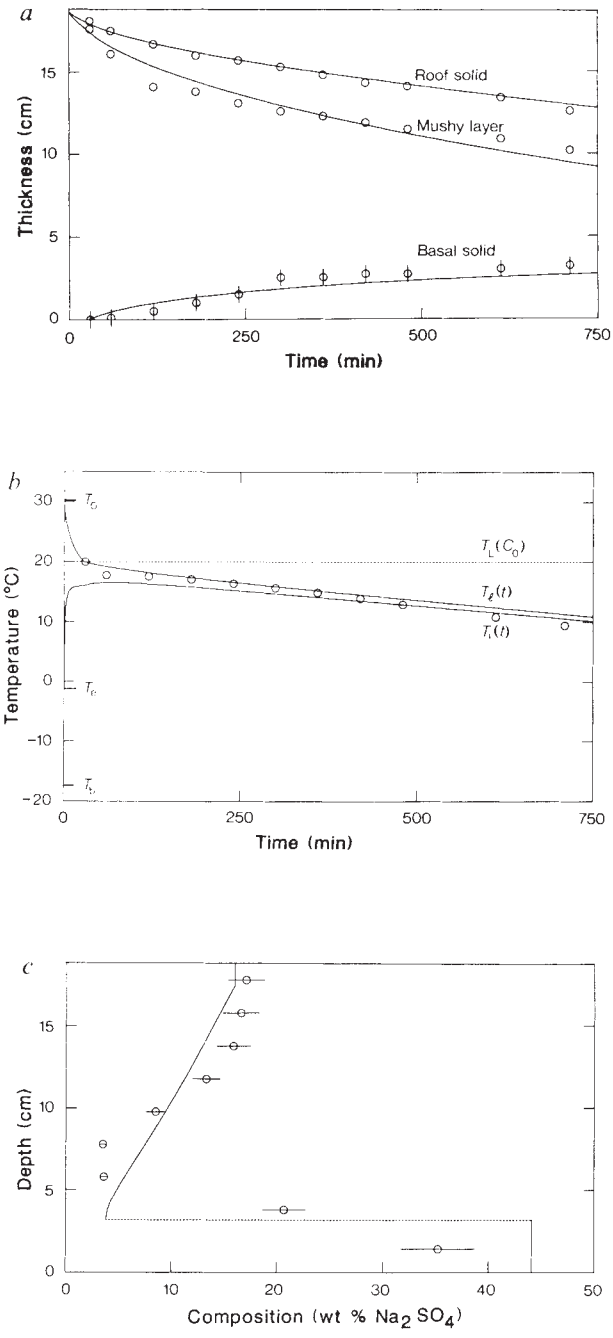

FIG. 5 *a*, The thickness of the roof solid $h_e(t)$ (upper curve) and mushy layer $h_i(t)$ (central curve) measured from the top of the container (height 18.8 cm) and the basal solid $h_f(t)$ (lower curve) measured from the floor of the tank for the complete solidification of an aqueous solution of sodium sulphate. Circles are experimental data. *b*, The temperature of the liquid $T_l(t)$ and of the mush–liquid interface $T_i(t)$ as functions of time. The circles show experimental values of the liquid temperature. (*c*), The compositional zonation of the final solid block as predicted by the theory and as measured in the experiment. Some error in the experimental values arises due to the melting of the solid while it is being cut into the 2-cm-thick horizontal sections for sampling. This has been indicated by the error bars. In the calculations $c_l = 4.1\ \mathrm{J\,cm^{-3}\,°C^{-1}}$, $c_\beta = 2.66\ \mathrm{J\,cm^{-3}\,°C^{-1}}$, $\mathscr{L}_\beta = 337\ \mathrm{J\,cm^{-3}}$, $\mathscr{L}_\alpha = 306\ \mathrm{J\,cm^{-3}}$, $\nu = 0.023\ \mathrm{cm^2\,s^{-1}}$, $k_l = 0.0059\ \mathrm{W\,cm^{-1}\,°C^{-1}}$, $k_\beta = 0.008\ \mathrm{W\,cm^{-1}\,°C^{-1}}$, $k_\alpha = 0.022\ \mathrm{W\,cm^{-1}\,°C^{-1}}$, $\lambda = 0.056$, $\alpha = (5.0 - (20 - T_l) \times 0.24) \times 10^{-4}\ \mathrm{°C^{-1}}$ where T_l in °C is the liquidus temperature of the melt. The eutectic point is $T_e = -1.2$ °C, $C_e = 3.8$ wt% Na_2SO_4 and the composition of the solid dendrites, made of $Na_2SO_4 \cdot 10\,H_2O$, is $C_\beta = 44.1$ wt% Na_2SO_4. The initial melt temperature and composition were 30.5 °C and 16 wt% Na_2SO_4. The liquidus curve for concentrations above C_e was calculated with a cubic spline by using data from ref. 24. The kinetic growth parameter used was $\mathscr{G} = 1.5 \times 10^{-4}\ \mathrm{cm\,s^{-1}\,°C^{-1}}$.

layer rises from T_b at $z=0$ to T_e at $z=h_e$. Below the eutectic front $z=h_e$, the system looks much as before: a stagnant mushy layer extends from $z=h_e$ to $z=h_i$ and lies above a convecting liquid region. Secondary crystals growing near the base of the container fill a depth h_f from the floor. This structure can be seen in the photographs in Fig. 4*a*, *b*. The eutectic front $z=h_e$ eventually reaches the base of the container, by which time the whole system is solidified. Once this had occurred in the experiments the whole solidified block, shown in Fig. 4*c*, was cut into horizontal sections and the bulk composition of each horizontal section was measured.

Figure 5 shows the results. Figure 5*c* shows that the mean composition decreases with depth from the top of the sample, which reflects the decreasing composition of the liquid region with time during the experiment. There is a jump in mean composition at the height where the interface between mush and liquid met the crystal layer growing up from the floor. The compositional discontinuity also marks a discontinuity in crystal morphology from vertically oriented dendritic crystals grown from the roof to randomly oriented smaller crystals grown at the floor. This is the so-called columnar-equiaxed transition, previously described by metallurgists[9]. Below this discontinuity the bulk composition is essentially uniform and equal to the composition of the pure component C_β. A smaller value of $\mathcal{G}$ than the one appropriate to the isopropanol system was needed to fit the data. This reflects the fact that crystals of sodium sulphate decahydrate are more faceted than ice crystals and require a greater supersaturation for a given growth rate.

Discussion

At a fundamental level the agreement between the results of our theoretical model and experiments validates our description of the mushy layer and its simulation as a continuum. There are many practical applications of this macroscopic approach to various situations considered by crystal growers and metallurgists, as discussed by Brice[10] and Brown[11]. There are also important geological applications, for example to the understanding of the cooling and solidification of lava flows. Basaltic lava lakes, cooled by the air[12], komatiitic lavas ponded on the sea floor[2] and magma chambers subject to hydrothermal cooling at the roof[13] are all examples in which the strongest cooling is from above and where the viscosity of the lava or magma is sufficiently low for them to convect turbulently. Equilibrium models of solidification will accurately predict the removal of any superheat from the lava and the initial formation of a dendritic crust. In such models, however, the crust buffers the interior of the lava from cooling below its initial liquidus temperature. By contrast, these models show that the coupling of fluid mechanical and disequilibrium effects can cause additional crystallization of the lava, either at the base of the flow or in its interior. This secondary solidification effects a change in the composition of the lava, which lowers the liquidus temperature and allows cooling and convection to continue.

In fact, turbulent convection can occur in a magma chamber even when there is no initial superheat. In such a case, before the onset of convection, both the depth of the mushy layer h and the thickness of the boundary layer below the mush-liquid interface δ, have magnitudes of order $(\kappa t)^{\frac{1}{2}}$, once the time elapsed since emplacement of the magma t is greater than $\tau_{\mathcal{G}}$. Accordingly, equation (13) shows that there is a kinetic undercooling ΔT of magnitude $\mathcal{G}^{-1}(\kappa/t)^{\frac{1}{2}}$. The local Rayleigh number based on δ and ΔT will exceed the critical value for convective instability Ra_c after a time of order $\tau_c=(\mathcal{G}\nu/\alpha g\kappa)\mathrm{Ra}_c$. If $\tau_c \ll \tau_\kappa$ there is sufficient time for breakdown of the boundary layer to generate turbulent convection in the melt. This condition is satisfied once the global Rayleigh number, based on the full depth of the chamber H and ΔT, is much greater than Ra_c, which is expressed by

$$\frac{\alpha g H^2}{\mathcal{G}\nu} \gg \mathrm{Ra}_c(\approx 10^3) \qquad (19)$$

A similar inequality was derived by Brandeis and Jaupart[14] for disequilibrium leading to nucleation of new crystals in the thermal boundary layer ahead of the solidification front. Alternatively, if there is some superheat initially such that the global Rayleigh number, based on H and the initial superheat, is sufficiently large then turbulent convection will occur even without the effects of disequilibrium[2].

Our study demonstrates further how the changing composition of the melt results in a stratification of the bulk composition of the mushy layer. It also provides a mechanism for the redistribution of solute during the complete solidification of an alloy cooled from above. Such macrosegregation is observed in completely solidified ingots and in igneous rocks[15].

We hope to extend our concepts to address more complicated and naturally realistic situations. For example, an additional geometrical dimension is introduced when the cooling and crystallization occurs at a side wall[16]. Horizontal temperature and compositional gradients drive a predominantly vertical flow adjacent to and through the mushy layer. Controlled experiments[17,18], in which cooling and crystallization took place at a sloping boundary, have shown dramatic differences between the forms of motion and crystallization at the upper and lower surfaces. The nature of the convection and its interaction with crystal growth would additionally be influenced by an initial stratification in the melt. Crystals and melt can interact in a fundamentally different way than considered here if the crystals are free to be swept along with any motion in the melt. Such systems have been called 'slurries'[19] in contrast to the mushy regions considered here. Further studies are under way to determine what portion of a slurry is mobile and what form of continuum mechanics, if any, is applicable to such flows. □

Received 23 January; accepted 13 June 1989.

1. Huppert, H. E. & Worster, M. G. *Nature* **314,** 703–707 (1985).
2. Turner, J. S., Huppert, H. E. & Sparks, R. S. J. *J. Petrology* **27,** 397–437 (1986).
3. Flemings, M. C. in *Modeling of Casting and Welding Processes* (eds Brody, H. D. & Arpelian, D.) 533–548 (The Metallurgical Society of the American Institute of Mining, Metallurgical and Petroleum Engineers, Warrendale, 1981).
4. Hills, R. N., Loper, D. E. & Roberts, P. H. *Q. Jl Mech. appl. Math.* **36,** 505–539 (1983).
5. Worster, M. G. *J. Fluid Mech.* **167,** 481–501 (1986).
6. Batchelor, G. K. *A. Rev. Fluid Mech.* **6,** 227–255 (1974).
7. Turner, J. S. *Buoyancy Effects in Fluids* (Cambridge University Press, 1979).
8. Kurz, W. & Fisher, D. J. *Fundamentals of Solidification* (Trans Tech Publications, Aedermannsdorf, 1986).
9. Flood, S. C. & Hunt, J. D. *Appl. Sci. Res.* **44,** 27–42 (1987).
10. Brice, J. C. *Crystal Growth Processes* (Blackie, Glasgow, 1986).
11. Brown, R. A. *A.I.Ch.E. Jl* **34,** 881–911 (1988).
12. Turcotte, D. L. & Schubert, G. *Geodynamics* (Wiley, New York, 1982).
13. Norton, D. & Taylor, H. P. *J. Petrology* **20,** 421–486 (1979).
14. Brandeis, G. & Jaupart, C. *Earth planet. Sci. Lett.* **77,** 345–361 (1986).
15. Shirley, D. N. *J. Petrology* **28,** 835–866 (1987).
16. Nilson, R. H. McBirney, A. R. & Baker, B. H. *J. Volcan. geotherm. Res.* **24,** 25–54 (1985).
17. Huppert, H. E., Sparks, R. S. J., Wilson, J. R. & Hallworth, M. A. *Earth planet. Sci. Lett.* **79,** 319–328 (1986).
18. Huppert, H. E., Sparks, R. S. J., Wilson, J. R., Hallworth, M. A. & Leitch, A. M. in *Origins of Igneous Layering* (ed. Parsons, I.) 539–568 (Reidel, Dordrecht, 1987).
19. Roberts, P. H. & Loper, D. E. in *Structure and Dynamics of Partially Solidified Systems* (ed. Loper, D. E.) 229–290 (Martinus Nijhoff, Dordrecht, 1987).
20. Abegg, R. *Z. phys. Chem.* **15,** 209–261 (1894).
21. Denton, R. A. & Wood, I. R. *Int. J. Heat Mass Transf.* **22,** 1339–1346 (1979).
22. Kaye, G. W. C. & Laby, T. H. *Tables of Physical and Chemical Constants and Some Mathematical Functions* (Longman, London and New York, 1973).
23. Vargaftik, N. B. *Tables on the Thermodynamic Properties of Liquids and Gases* (Wiley, New York, 1975).
24. Washburn, E. W. (ed.) *International Critical Tables of Numerical Data: Physics, Chemistry and Technology* (McGraw-Hill, New York and London, 1926).
25. Weast, R. C. (ed.) *CRC Handbook of Chemistry and Physics* (Chemical Rubber Co., Cleveland, 1971).

ACKNOWLEDGEMENTS. We thank Mark Hallworth for his technical assistance. Helpful comments on an earlier draft were given to us by J. A. Dantzig, C. Donaldson, D. T. J. Hurle and C. Jaupart. We gratefully acknowledge research fellowships from the following Cambridge Colleges: Churchill (R.C.K.), St John's (A.W.W.) and Trinity (M.G.W.) and also the financial support of the B.P. Venture Research Unit (H.E.H.).